ACS APPLIED MATERIALS & INTERFACES

Research Article

www.acsami.org

Improved Langmuir–Blodgett Titanate Films via in Situ Exfoliation Study and Optimization of Deposition Parameters

Huiyu Yuan, Roy Lubbers, Rogier Besselink, Maarten Nijland, and Johan E. ten Elshof*

MESA+ Institute for Nanotechnology, University of Twente, P.O. Box 217, 7500 AE Enschede, The Netherlands

Supporting Information

ABSTRACT: The exfoliation and deposition of large (10–100 μm) $Ti_{0.87}O_2$ and small (0.1–1 μm) $Ti_{0.91}O_2$ nanosheets from lepidocrocite-type protonated titanates was investigated for getting high quality films. Exfoliation was carried out with different tetra-alkyl ammonium ions (TAA^+) and varying TAA^+/H^+ ratios, and the colloidal solutions were characterized by small-angle X-ray scattering (SAXS) and ultraviolet–visible (UV–vis) spectroscopy. Using Langmuir-Blodgett deposition the titanate nanosheets were directly transferred onto a Si substrate. The resulting films were characterized by atomic force microscopy (AFM).The results indicate that the $H_{1.07}Ti_{1.73}O_4$ titanate exfoliated at very low ratios of TAA^+/H^+; no lower threshold for exfoliation was observed for the TAA^+ concentration. Nanosheets exfoliated at very low ratios of TAA^+/H^+ typically showed a small size and porous surface. Subsequent exfoliation of the remaining layered titanate particles yielded much higher quality nanosheets. The optimized deposition parameters for Langmuir-Blodgett films suggest that the surface pressure is a key parameter to control the coverage of the film. The bulk concentration of nanosheets was found to be a less important deposition parameter in the LB deposition process. It only influenced whether the desired surface pressure could be reached at a given maximum degree of compression.

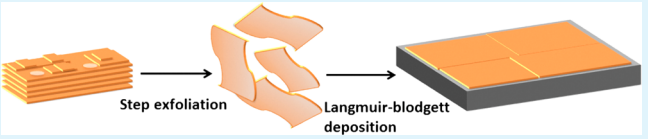

KEYWORDS: *titanate, nanosheets, Langmuir–Blodgett deposition, exfoliation, tetraalkylammonium*

INTRODUCTION

Two-dimensional (2D) materials such as graphene are attracting much attention because of their interesting properties, which are quite distinct from three-dimensional materials.[1−7] Among the 2D materials, graphene is the most thoroughly studied one.[2] However, besides graphene a large number of other 2D materials exists, which are prepared from three-dimensional precursor crystals that have strong covalent or ionic in-plane bonds and weak out-of-plane van der Waals bonds.[8−10] Those 2D materials are a source of novel advanced materials and they may offer a huge opportunity to design new or downscaled functionalities.[10,11] In particular, because of their 2D nature and semiconducting characteristics, oxide nanosheets are regarded as a promising new channel material in field effect transistors and molecular electronics, e.g. titania.[11] Titania nanosheets have been studied intensively in recent years.[12−16] They are commonly derived from $H_{0.7}Ti_{1.825}O_4$ (denoted further as HTO-1) or $H_{1.07}Ti_{1.73}O_4$ (denoted further as HTO-2) by means of a so-called exfoliation or delamination process.[14,15] Essentially, protonated layered titanates are mixed with tetraalkylammonium hydroxides (TAAOH) in aqueous solution, and the layered oxides are exfoliated via spontaneous intercalation of tetraalkylammonium ions (TAA^+) into the adjacent layers via ion exchange with protons.[15,17] This technique gives large quantities of dispersed nanosheets and may be a promising method to make novel types of 2D nanoobjects that can be incorporated into functional thin films and composites.[18,19] The $Ti_{0.91}O_2$ and $Ti_{0.87}O_2$ nanosheets exfoliated from HTO-1 and HTO-2, respectively, have largely different lateral sizes. The lateral sizes of the $Ti_{0.87}O_2$ nanosheets ranged from 10 to 100 μm,[15] and are 2 orders of magnitude larger than the sizes of $Ti_{0.91}O_2$ nanosheets, which ranged from 0.1 to 1 μm.[20] The difference is mainly due to the fact that $K_{0.80}Ti_{1.73}Li_{0.27}O_4$ (denoted further as KLTO), the parent compound for HTO-2 and ultimately $Ti_{0.87}O_2$, was prepared in a liquid flux, while $Cs_{0.7}Ti_{1.825}O_4$ (denoted further as CTO), the parent compound for HTO-1 and $Ti_{0.91}O_2$, was made by conventional solid state reaction.

Sasaki et al. studied the exfoliation of HTO-1 by means of X-ray diffraction and UV-visible light absorption spectroscopy.[14] They concluded that a molar ratio TBA^+/H^+ (where H^+ refers to the protons in the protonated titanate, in this case in $H_{0.7}Ti_{1.825}O_4$) of approximately 0.3–0.5 presented a threshold for exfoliation, below which only the usual intercalation reaction occurred. They also studied restacking of exfoliated titanates and found that drying of the colloids brings about spontaneous reassembly of the nanosheets into layered hybrid materials.[21] We studied the exfoliation and restacking of layered titanates in solution and found that the restacking of titania nanosheets is controlled by electrostatic interactions due to the presence of a diffuse double layer of positively charged ions between negatively charged nanosheets. The interlayer spacing is controlled by the double layer thickness.[16] Recently, Maluangnont et al. studied the difference between exfoliation

Received: March 10, 2014
Accepted: May 12, 2014
Published: May 12, 2014

   dx.doi.org/10.1021/am501380d | ACS Appl. Mater. Interfaces 2014, 6, 8567–8574

and restacking of protonated layered titanates (HTO-2) by tetramethylammonium hydroxide (TMAOH) and tetrabutylammonium hydroxide (TBAOH) with a molar ratio $TAA^+/H^+ > 0.5$, and found that the lateral size of the nanosheets could be controlled, depending on the type of cation, by the TAA^+/H^+ molar ratio, and the mode of the exfoliation process (manual versus mechanical shaking).[22] So the colloidal state of nanosheets exfoliated in solution is very sensitive to its chemical environment. In situ measurements would therefore offer a better way to study the exfoliation of nanosheets.

Langmuir-Blodgett (LB) deposition has been shown a useful technique to transfer oxide nanosheets from the liquid phase to a solid substrate and form dense monolayer films.[23−28] It is widely applicable to hydrophilic substrates such as quartz, silicon, indium−tin oxide (ITO) and glass, but also to hydrophobic Au.[27] Highly ordered nanosheet thin films have been obtained by controlling the LB deposition process.[23,28] However, LB deposition has not been used to study the influence of parameters like the nature of TAA^+ and the molar ratio TAA^+/H^+ on exfoliation. Although efforts have been made to study the effect of LB deposition parameters such as surface pressure and suspension concentration on the formation of nanosheet monolayers,[27] little work was systematically focusing on the relationship between those parameters and the morphology and coverage of monolayer nanosheet films.

In the present paper we chose HTO-2 as a model compound to study the influence of the molecular size of TAA^+ and the ratio TAA^+/H^+ on the exfoliation process, because of the big $Ti_{0.87}O_2$ nanosheets it provides. By using LB deposition and Atomic Force Microscopy (AFM) the exfoliated nanosheets from solution could be visualized directly. We employed $Ti_{0.91}O_2$ and $Ti_{0.87}O_2$ nanosheets to study the relationship between the main LB deposition parameters, namely surface pressure and nanosheet bulk concentration, on the density and structure of the resulting monolayer film on silicon substrates. Our goal is to understand and control the process of formation of reproducible high-quality nanosheet monolayers and multilayer films with coverage close to 100%.

EXPERIMENTAL SECTION

Materials. Titanium(IV) dioxide TiO_2 (Ridel-de Haen), molybdenum(VI) oxide MoO_3 (Sigma-Aldrich), anhydrous potassium carbonate K_2CO_3 (Fluka), lithium carbonate Li_2CO_3 (Ridel-de Haen), and cesium carbonate Cs_2CO_3 (Sigma-Aldrich) had a purity of 99.0% or higher and were used as received. Tetra *n*-methylammonium hydroxide pentahydrate TMAOH (97%, Acros Organics), tetra *n*-ethylammonium hydroxide TEAOH (35 wt % in H_2O, Sigma-Aldrich), tetra *n*-propylammonium hydroxide TPAOH (1.0 M in H_2O, Sigma-Aldrich), and tetra *n*-butylammonium hydroxide TBAOH (40 wt % H_2O, Alfa Aesar) were used as received. Demineralized water was used throughout the experiments.

Preparation of Lepidocrocite-Type Protonated Layered Titanates. The CTO precursor was prepared according to the solid state synthesis procedure described elsewhere.[29] In a typical synthesis procedure, a mixture of Cs_2CO_3 and TiO_2 in 1:5.3 molar ratio was heated to 800 °C and kept for 20 h. The resulting CTO powder was dispersed in 2 mol/L HNO_3 to exchange Cs^+ ions by H_3O^+ ions. Protonation was conducted for 3 days by refreshing the acidic solution every day. Then the resulting powder was washed with water to remove residual acid, filtered and dried in air to obtain crystals of HTO-1.

The KLTO precursor was obtained with a flux method developed by Tanaka et al.[15] TiO_2, K_2CO_3, Li_2CO_3, and MoO_3 (1.73:1.67:0.13:1.27 molar ratio) were heated to 1150°C, held at that temperature for 30 min, and then slowly cooled down to 950 °C at a speed of 4 °C/h. The oven was then allowed to cool to room temperature by natural cooling. The resulting KLTO powder was washed 3 times in 250 mL water to remove K_2MoO_4. Then KLTO powder was dispersed in a 2 mol/L HNO_3 solution (250 mL) at room temperature while stirring. The acidic solution was replaced daily by a fresh one by decantation. After treatment for 3 days, the acid-exchanged crystals were collected by filtration and washed with a copious quantity of pure water, then air-dried to get HTO-2 powder.

Preparation of TAA^+-Titanate Solutions. For UV-visible absorption and Small Angle X-ray Scattering (SAXS) experiments, samples were made by mixing 0.5 g of HTO-2 with water and TMAOH, TEAOH, TPAOH or TBAOH, respectively, with a TAA^+/H^+ (HTO-2) molar ratio of 1:32, 1:16, 1:8, 1:4, 1:2, or 1:1 to a total volume of 100 mL solution. The fixed mixing sequence was HTO-2, water and then TAAOH. The mixtures were mechanically shaken (60 rpm) for 7 days. Then the solutions were kept standing for 3 days after which the suspensions were collected. To avoid breaking the nanosheets,[22] surfactant devoid solutions for LB deposition were prepared separately with the same procedure but on a shaking plate at a rate of 30 rpm in a soft way. The colloidal suspensions from HTO-1 and HTO-2 for LB deposition study were mixed with TBAOH on a shaking plate with a frequency of 30 rpm for 7 days. The molar ratio of TBA^+/H^+ (where H^+ refers to $H_{0.7}Ti_{1.825}O_4$ or $H_{1.07}Ti_{1.73}O_4$) was kept constant at 1. After 7 days, the resulting suspensions were kept standing for 1 day, and then the suspensions were used for LB deposition.

Langmuir−Blodgett Deposition. The deposition suspensions were prepared from stock suspensions of the solution. A defined quantity of stock solution was diluted 20 times by volume to obtain a deposition suspension. The diluted suspensions were then left standing for 1 day. For LB deposition, 50 mL was separated from the middle/top part of the nanosheet suspension by using a syringe. The separated suspension was poured into a Langmuir Blodgett trough (KSV Minimicro, a Teflon trough with an active trough surface area of 100 cm^2, L195 x W51 x D4 mm^3 and a dipping well of L10 × W28 × D28 mm^3, trough volume 48 cm^3) and left for 15 min to equilibrate and stabilize the surface pressure before the deposition process was started. Generally a film was deposited at a surface pressure of 10 mN/m unless otherwise stated. The trough was cleaned prior to every experiment with ethanol and a soft brush, rinsed several times with distilled water to remove ethanol, and then blown dry with nitrogen.

The silicon substrate was first cleaned with a CO_2 snow jet to remove dust particles and adsorbates. Then, it was cleaned in a Harrick Plasma PDC-002 oxygen plasma cleaner (25 W) for 5 min to oxidize any residual organic residues on the substrate surface. Subsequently, the silicon substrate was immersed vertically into the suspension. The surface pressure was measured using a Wilhelmy plate attached to the KSV Minimicro frame.

Characterization. UV-Vis spectra for samples were recorded with a Cary 50 UV-Vis spectrophotometer in transmission mode. The original suspensions were diluted 333 times by volume to obtain an appropriate range of absorbances. SAXS experiments were carried out using synchrotron radiation on the Dutch-Belgian beamline, DUBBLE BM-26B of the European Synchrotron Radiation Facility (ESRF) in Grenoble.[30] The colloidal samples were placed in capillary glass tubes (Hilgenberg no. 14, dimensions: 80 mm length; 1.5 mm diameter; wall thickness ~10 μm).[16] Tapping mode Atomic Force Microscopy (AFM; Veeco Dimension Icon) was used to determine the height profile of nanosheets deposited on Si wafers. The AFM data were further analyzed using the Gwyddion (version 2.31) software package. The coverage of the substrate by nanosheets was determined using ImageJ software. The analysis was based on manually set thresholds for contrast and brightness. The coverage can be calculated from the color difference between substrate and areas occupied area by nanosheets. Details can be found in the Supporting Information.

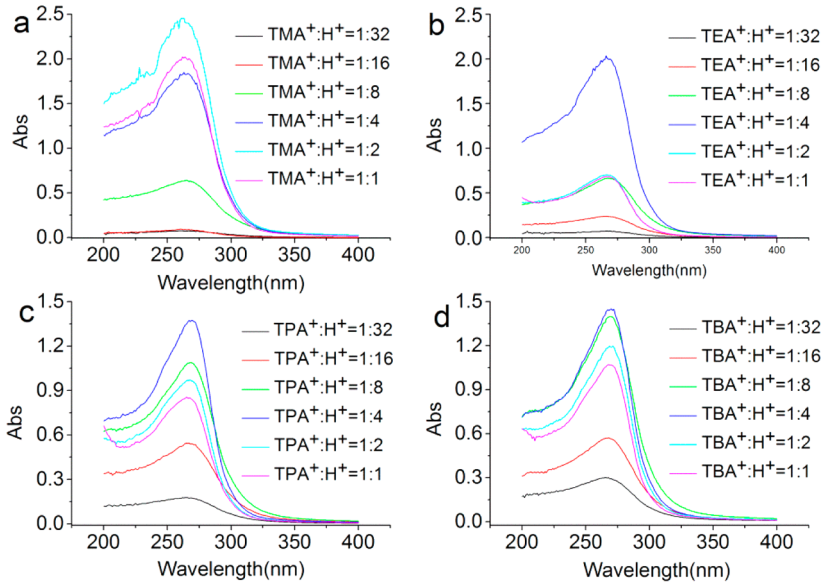

Figure 1. UV−visible spectra of diluted HTO-2 suspensions at different TAA^+/H^+ molar ratios.

RESULTS AND DISCUSSION

Influence of Molecular Size of TAA^+ and Molar Ratio TAA^+/H^+ on Exfoliation. Figure 1 shows the optical absorption spectra of colloidal suspensions at different TAA^+/H^+ (HTO-2) molar ratios. The absorption peak is located at a wavelength of 265 nm, which was blue-shifted in comparison to the absorption peak of bulk anatase TiO_2 and HTO-1.[14,23,28,31] This phenomena indicates the effect of 2D quantum confinement due to the nanosized dimensions of the nanosheets in one direction. According to the Lambert-Beer law, the absorbance should increase linearly with the concentration of nanosized titanates in the suspensions. For the samples with low molar ratios of 1:32 and 1:16, the absorbance appeared to depend more on the nature of the quaternary ammonium ion than on its concentration. The results show that as the size of TAA^+ increases the peak absorbance increases. For the sake of clarity, the peak absorbances are plotted in Figure 2.

Care should be taken to compare absolute values between different TAAOH suspensions with similar TAA^+/H^+ ratio.

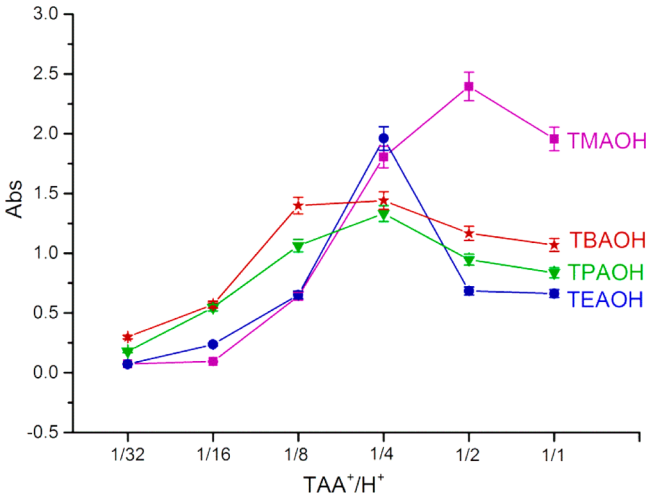

Figure 2. Absorbance of diluted suspensions at TAA^+/H^+(HTO-2) molar ratios of 1:32 to 1:1.

However, trends with varying TAA^+/H^+ ratio can be compared directly for a given type of TAAOH. For TMAOH and TEAOH, a considerable concentration of nanosized titanates was only obtained at a molar ratio above 1:16. For TPAOH and TBAOH, the ratio of 1:32 led already to a substantial concentration of nanosheets. Furthermore, except for the TMA^+ based suspension, the maximum absorbance of other suspensions with larger TAA^+ ions was observed with a TAA^+/H^+ molar ratio of 1:4. At molar ratios above 1:4 the intensity was lower, which probably means that some restacking of nanosheets occurred. It is noteworthy that HTO-2 behaved differently from HTO-1, which did not show any restacking at TBA^+/H^+ molar ratios between 0.1 and 1.[14] This may be due to the small size of HTO-1 derived nanosheets, which may decrease the chance that nanosheets coagulate. Meanwhile, suspensions with a molar ratio 1:1 showed a small absorption increase near 200 nm wavelength, but suspensions with a molar ratio 1:2 did not. This feature is an indication of free hydroxide ions in the suspensions.[32,33] The reason for the presence of this absorption peak at a TAA^+/H^+ molar ratio of 1:1 is the proton deficient nature of HTO-2.[34] Finally, it is noted that TMAOH behaved somewhat differently than the others. For TMAOH the highest absorption was observed at a TMA^+/H^+ molar ratio of 1:2, the other TAA^+ ions showed maxima at around 1:4. The trend may be related to the variation in TAA^+ size.

Hence, the UV−visible absorption spectra confirmed the presence of nanosized particles in the suspensions at low TAA^+/H^+ molar ratio. In order to investigate the structure of these nanosized particles, SAXS experiments were performed on colloidal suspensions. The results are shown in Figure 3.

The SAXS curves from the TMA^+-titanate system and the TEA^+-titanate system showed a small correlation peak at q = 1.0 nm^{-1} at TAA^+/H^+ molar ratios higher than 1:4. This indicates that a low concentration of layered structures was present in these suspensions. The absence of similar pseudo-Bragg peaks in the SAXS data of the TPA^+-titanate and the TBA^+-titanate system indicated that the nanosized titanates in these colloidal suspensions were not layered but were present only as isolated sheets. It is noteworthy that restacking occurred at TAA^+/H^+ molar ratios above 1:4 irrespective of the nature of

dx.doi.org/10.1021/am501380d | ACS Appl. Mater. Interfaces 2014, 6, 8567−8574

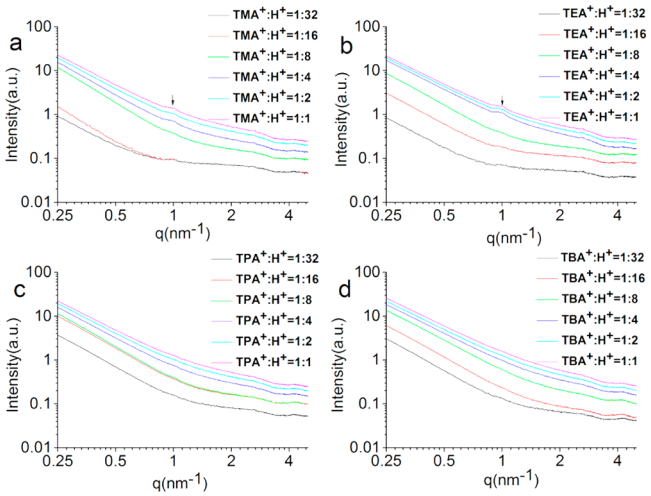

Figure 3. SAXS profiles for the colloidal HTO-2 suspensions at different TAA^+/H^+ ratios.

TAA^+ (see the Supporting Information File, Figure S2). This observation is in agreement with the reduction of absorbance in the UV-visible data at high TAA^+/H^+ ratio. However, only the TMA^+-titanate system and the TEA^+-titanate system showed a correlation peak at q = 1.0 nm^{-1} after sedimentation for 3 days. This result indicates that the TMA^+-titanate system and the TEA^+-titanate system tend to restack but disperse stably without precipitation at high concentration after an extended period of time (3 days). In contrast, these systems do not remain stable and agglomerate at low concentration within a short time period (24 h), based on our experimental observation in LB deposition as described below.

We attempted to make Langmuir–Blodgett films of nanosheets from these suspensions by using different TAA^+-titanate suspensions with TAA^+/H^+ of 1:4. The stock suspensions with a TAA^+/H^+ molar ratio of 1:4 were diluted 20 times by volume. Unfortunately, the TMAOH and TEAOH based suspensions aggregated after 1 day standing, and the concentration appeared to be insufficient to make a good LB film. The maximum surface pressure that could be obtained after 60% compression for TMAOH and TEAOH based suspensions was less than 2 mN/m. However, isolated nanosheets were found on the substrate (see Figure 4a, b). On the other hand, good quality films were obtained from TPAOH and TBAOH based suspensions (see Figure 4c, d). The nanosheets revealed by AFM were ∼1.2 nm thick, which corresponds well with values of titanate nanosheets reported elsewhere.[15,20]

Based on the UV-visible spectra of the TBA^+/H^+ (HTO-2) system shown in Figure 1d, the concentration of isolated nanosheets at a TBA^+/H^+ ratio of 1:16 was significantly high. A LB deposition process was therefore performed using an HTO-2 suspension with a TBA^+/H^+ ratio of 1:16. The corresponding AFM image can be found in Figure 5a, b. The AFM results confirm the presence of pores within the nanosheets. In addition, many agglomerated nanoparticles were present. It is worth to note that a large amount of unreacted HTO powder was found on the bottom of the reaction bottle. After removal of the exfoliated nanosheet suspension, further exfoliation and LB deposition was conducted using these unreacted HTO particles. The corresponding AFM images of nanosheets from the second exfoliation process can be found in Figure 5c, d. It can be seen that the average size of the nanosheets in this film is much larger than in Figure 5a. Moreover, porosity was absent in these nanosheets. So although exfoliation of titanate nanosheets occurred at very low TAA^+/H^+ ratio, yielding sufficiently high concentrations of nanosheets to allow deposition of a LB film, the quality of the initial nanosheets was much lower than that of the nanosheets from subsequent exfoliation processes.

Steric hindrance is considered to have a key influence on the delamination rate of layered materials.[14,35] The surface of the nanosheets shown in Figure 5a is very porous (see detail image in Figure 5b), which means that diffusion of ions into these layered oxides, and the exchange of protons and TAA^+ was probably faster than in stacked nanosheets with more intact titanate layers. As it was previously determined the individual nanosheets in the layered protonated titanate are connected through strong hydrogen bonds.[34] It is reasonable to assume

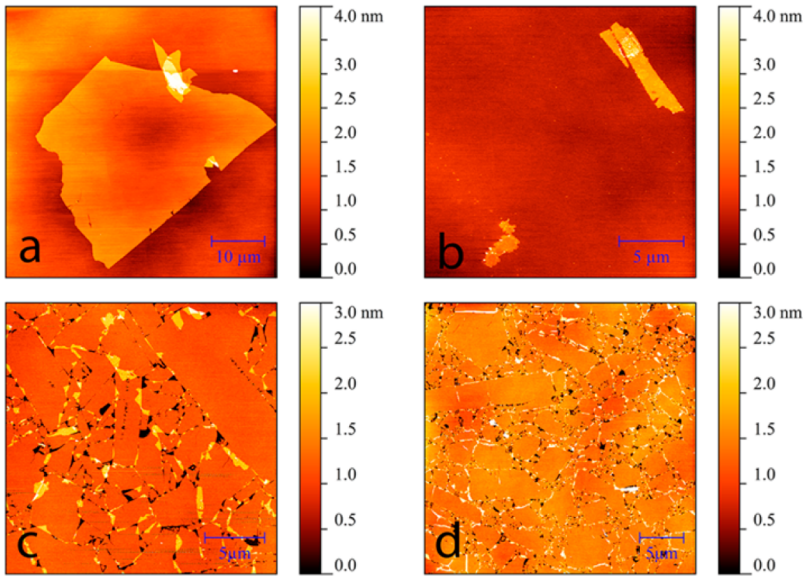

Figure 4. AFM images of LB deposited HTO-2 derived nanosheet films obtained by different types of TAAOH at constant TAA^+/H^+ ratio of 1:4. (a) TMA^+/H^+; (b) TEA^+/H^+; (c) TPA^+/H^+; (d) TBA^+/H^+.

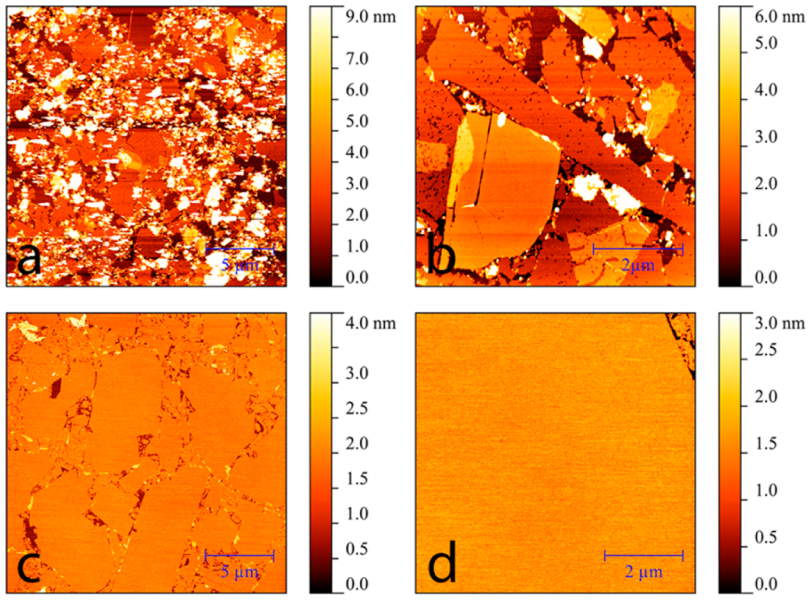

Figure 5. AFM images of LB nanosheet films obtained from a suspension with TBA^+/H^+(HTO-2) = 1:16. (a) Nanosheets from first exfoliation process; (b) magnified image of nanosheets from first exfoliation, showing porous nanosheets; (c) nanosheets from second exfoliation process; (d) magnified image of nanosheets from second exfoliation.

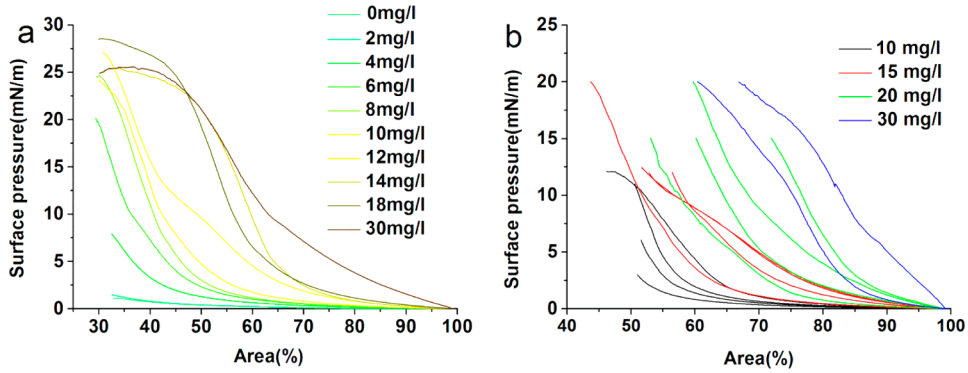

Figure 6. Surface pressure−surface area curves of (a) a $Ti_{0.91}O_2$ nanosheet suspension from HTO-1 (small sheets) and (b) a $Ti_{0.87}O_2$ nanosheet suspension from HTO-2 (large sheets).

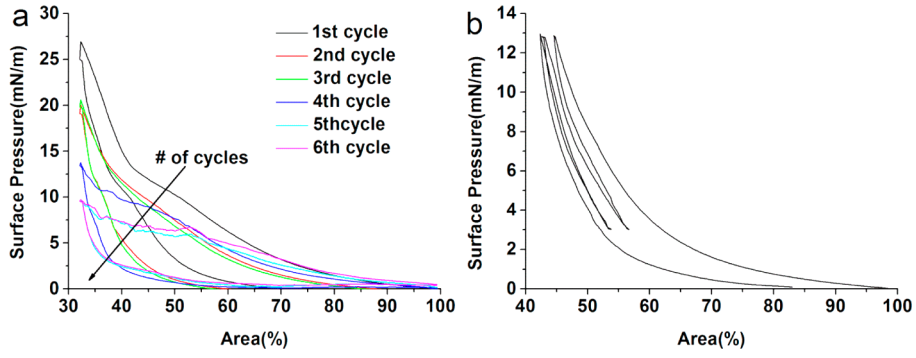

Figure 7. Surface pressure−surface area compression-expansion curves of (a) $Ti_{0.91}O_2$ (12 mg/L) nanosheet suspensions upon repetitive compression to 30% and expansion to 100%; (b) $Ti_{0.91}O_2$ (12 mg/L) nanosheet suspensions upon repetitive experiments (surface pressure: 0→ 13 → 3→13 → 3→13 → 0 mN/m).

that the exfoliation only occurs after these hydrogen bonds are broken through a reaction between protons and hydroxide ions that were diffusing into HTO from the solvent matrix. For porous and small nanosheets the diffusion path for hydroxide and TAA^+ ions is shorter than with nanosheets without pores and with big nanosheets. So nanosheets with many pores and small nanosheet stacks are expected to be exfoliated faster than those without pores and big nanosheets. Hence, small and porous nanosheets are probably most sensitive to exfoliation and can be obtained at low TAA^+/H^+ ratio, in qualitative agreement with the morphology shown in Figure 5.

dx.doi.org/10.1021/am501380d | ACS Appl. Mater. Interfaces 2014, 6, 8567−8574

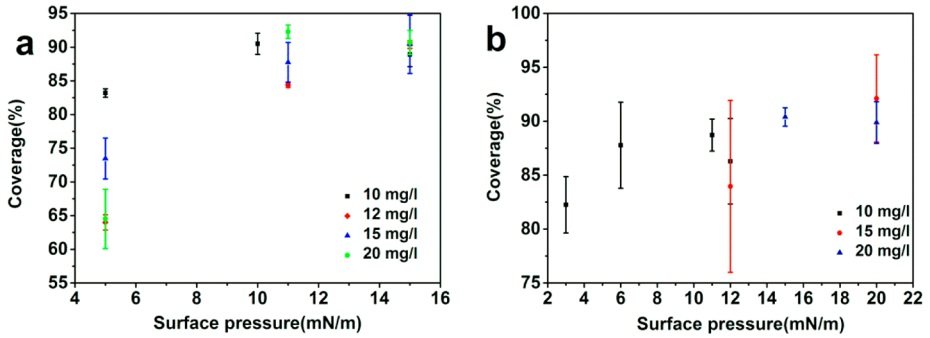

Figure 8. Coverage of substrate by nanosheets (%) versus surface pressure for (a) $Ti_{0.91}O_2$ bulk concentrations of 10−20 mg/L; (b) $Ti_{0.87}O_2$ bulk concentrations of 10−20 mg/L.

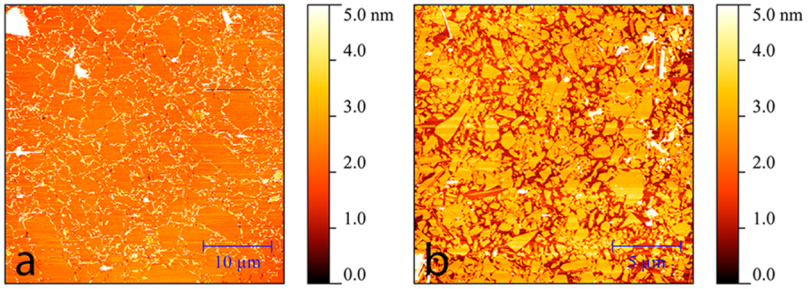

Figure 9. (a) $Ti_{0.87}O_2$ film (suspension concentration 30 mg/L, surface pressure 20 mN/m) at 97% coverage; (b) $Ti_{0.91}O_2$ film (suspension concentration 20 mg/L, surface pressure 5 mN/m) at 63% coverage.

Influence of Surface Pressure and Nanosheet Concentration on Formation of Monolayer Nanosheet Thin Film. Surface pressure−surface area compression curves of $Ti_{0.91}O_2$ and $Ti_{0.87}O_2$ nanosheet suspensions with different concentrations were made to investigate the relationship between surface pressure and bulk nanosheet concentration. See Figure 6. The numbers in Figure 6 are based on the nominal 1.5 g/L HTO-1 and HTO-2 stock suspensions, which were diluted to 400 mg/L. The diluted suspension can be regarded as a pure sub-phase on which no nanosheets are present at the liquid−air surface without compression. The bulk concentration of both $Ti_{0.91}O_2$ and $Ti_{0.87}O_2$ nanosheets in the dipping solution has a clear influence on the trend in the surface pressure upon compression. Solutions with higher bulk concentrations needed less compression to achieve a certain surface pressure. For $Ti_{0.91}O_2$ nanosheets, until a bulk concentration of 6 mg/L no maximum in the surface pressure was observed upon 70% compression. At higher bulk concentrations, the surface pressure appeared to saturate at values of 25-28 mN/m at 70% compression. This result agrees well with the data reported by Yamaki et al., who found that a pressure of ∼25 mN/m was the saturated point of $Ti_{0.91}O_2$ nanosheets.[24] For the much larger $Ti_{0.87}O_2$ nanosheets the reproducibility was poor, as illustrated in Figure 6b where several compression curves are shown for each bulk composition. The poor reproducibility is likely related to the wide size distribution of the $Ti_{0.87}O_2$ nanosheets.

Compression-expansion experiments were conducted in a Langmuir trough to determine to what extent the LB compression process is reversible for nanosheets. Several repetitive compression and expansion cycles were conducted at several bulk concentrations. Figure 7a shows the surface pressure upon compression to 30% and subsequent expansion to 100% of a $Ti_{0.91}O_2$ suspension with a moderate bulk concentration of 12 mg/L. After every compression cycle the maximum attained surface pressure at a given degree of compression was lower than in the previous cycle, and the qualitative resemblance with a "classical" surface pressure isotherm of a diluted aqueous surfactant was lost. The same trends were also observed at all other concentrations. The decreasing maximum surface pressure after each compression cycle to 30% (Figure 7a) was likely caused by agglomeration or restacking of monolayer nanosheets. However, when the suspension was compressed to a lower maximum surface pressure (i.e. less compression), the expansion was less irreversible, as illustrated in Figure 7b for a series of compression and expansion cycles. This can be explained that upon compression a rigid monolayer film formed at the air−water interface, and without enough relaxation time this monolayer is known to stay intact.[27]

Nanosheets were transferred to silicon substrates to investigate the coverage at different nanosheet bulk concentrations and surface pressures. Panels a and b in Figure 8 show the coverages of a silicon substrate by $Ti_{0.91}O_2$ and $Ti_{0.87}O_2$ nanosheets as a function of the nanosheet bulk concentration and surface pressure. To determine the coverages, at least 3 AFM images of almost every sample were analyzed.

For both $Ti_{0.91}O_2$ and $Ti_{0.87}O_2$ nanosheets, the coverages increased with increasing surface pressure. However, the surface roughened when a very high surface coverage was reached. Figure 9a shows a high coverage (97%) film of $Ti_{0.87}O_2$ nanosheets and Figure 9b a low coverage (63%) film of $Ti_{0.91}O_2$ nanosheets. The bright areas are indicative of nanosheet stacking and film roughening effects. However, the overlap can be trimmed to get a high-coverage and well-organized film.[23,28] It is noted that the nanosheets were thoroughly attached to the silicon substrate after deposition.

Treatment with a CO_2 snow jet at a pressure of 25−50 bar did not result in a significant change in coverage.

CONCLUSIONS

The concentration of nanosized titanates formed in a suspension is related to the nature of TAAOH at low ratios of TAA^+/H^+ for HTO-2. Exfoliation occurred already at very low ratios of TAA^+/H^+; no lower threshold of exfoliation for the TAA^+ concentration was observed. Nanosheets exfoliated from an HTO suspension with a low ratio TAA^+/H^+ of 1:16 showed many pores on their surfaces, indicating that these sheets were exfoliated first. Higher quality, intact nanosheets were exfoliated at a later stage from the parent crystals. A two-step exfoliation procedure in which first the defective nanosheets are removed at low TAA^+/H^+ ratio, followed by a second separate exfoliation step in which the rest of the crystals is exfoliated aid in obtaining higher quality LB films of nanosheets. The bulk concentration of nanosheets was found to be a less important deposition parameter in the LB deposition process. It only influenced whether the desired surface pressure could be reached at a given maximum degree of compression. The higher the bulk concentration, the less compression was required to achieve a given surface pressure. By using high surface pressure, the high coverage nanosheet films, >95%, were achieved. However, a too high surface pressure leads to overlap, stacking and clustering of nanosheets at the liquid surface, resulting in roughened films.

ASSOCIATED CONTENT

Supporting Information

Details of substrate coverage determination, and SAXS data of the colloidal HTO-2 suspensions without sedimentation at different TAA^+/H^+ ratios. This material is available free of charge via the Internet at http://pubs.acs.org.

AUTHOR INFORMATION

Corresponding Author

*E-mail: j.e.tenelshof@utwente.nl.

Author Contributions

The manuscript was written through contributions of all authors. All authors have given approval to the final version of the manuscript.

Notes

The authors declare no competing financial interest.

ACKNOWLEDGMENTS

The authors acknowledge the financial support of the Chemical Sciences division of The Netherlands Organization for Scientific Research (NWO−CW) and the program of China Scholarships Council (CSC, No.2011704003). We thank The Netherlands Organization for Scientific Research (NWO) for beam time at the ESRF DUBBLE beamline. We thank Dr. G. Portale, Dr. D. Hermida Merino and Dr. W. Bras from DUBBLE for on-site assistance and useful discussions. We thank M.Sc P. Gonzalez Rodriguez and Ing. S. Veldhuis for any assistance during SAXS measurement.

REFERENCES

(1) Castro Neto, A. H.; Guinea, F.; Peres, N. M. R.; Novoselov, K. S.; Geim, A. K. The Electronic Properties of Graphene. *Rev. Mod. Phys.* **2009**, *81*, 109−162.

(2) Geim, A. K.; Novoselov, K. S. The Rise of Graphene. *Nat. Mater.* **2007**, *6*, 183−191.

(3) Xia, F.; Mueller, T.; Lin, Y.-m.; Valdes-Garcia, A.; Avouris, P. Ultrafast Graphene Photodetector. *Nat. Nanotechnol.* **2009**, *4*, 839−843.

(4) Ueno, K.; Nakamura, S.; Shimotani, H.; Ohtomo, A.; Kimura, N.; Nojima, T.; Aoki, H.; Iwasa, Y.; Kawasaki, M. Electric-field-induced Superconductivity in an Insulator. *Nat. Mater.* **2008**, *7*, 855−858.

(5) Stankovich, S.; Dikin, D. A.; Dommett, G. H. B.; Kohlhaas, K. M.; Zimney, E. J.; Stach, E. A.; Piner, R. D.; Nguyen, S. T.; Ruoff, R. S. Graphene-based Composite Materials. *Nature* **2006**, *442*, 282−286.

(6) Novoselov, K. S.; Geim, A. K.; Morozov, S. V.; Jiang, D.; Katsnelson, M. I.; Grigorieva, I. V.; Dubonos, S. V.; Firsov, A. A. Two-dimensional Gas of Massless Dirac Fermions in Graphene. *Nature* **2005**, *438*, 197−200.

(7) Novoselov, K. S.; Geim, A. K.; Morozov, S. V.; Jiang, D.; Zhang, Y.; Dubonos, S. V.; Grigorieva, I. V.; Firsov, A. A. Electric Field Effect in Atomically Thin Carbon Films. *Science* **2004**, *306*, 666−669.

(8) Mas-Balleste, R.; Gomez-Navarro, C.; Gomez-Herrero, J.; Zamora, F. 2D Materials: to Graphene and Beyond. *Nanoscale* **2011**, *3*, 20−30.

(9) Butler, S. Z.; Hollen, S. M.; Cao, L.; Cui, Y.; Gupta, J. A.; Gutiérrez, H. R.; Heinz, T. F.; Hong, S. S.; Huang, J.; Ismach, A. F.; Johnston-Halperin, E.; Kuno, M.; Plashnitsa, V. V.; Robinson, R. D.; Ruoff, R. S.; Salahuddin, S.; Shan, J.; Shi, L.; Spencer, M. G.; Terrones, M.; Windl, W.; Goldberger, J. E. Progress, Challenges, and Opportunities in Two-Dimensional Materials Beyond Graphene. *ACS Nano* **2013**, *7*, 2898−2926.

(10) Geim, A. K.; Grigorieva, I. V. Van der Waals Heterostructures. *Nature* **2013**, *499*, 419−25.

(11) Osada, M.; Sasaki, T. Exfoliated Oxide Nanosheets: New Solution to Nanoelectronics. *J. Mater. Chem.* **2009**, *19*, 2503−2511.

(12) Sasaki, T.; Nakano, S.; Yamauchi, S.; Watanabe, M. Fabrication of Titanium Dioxide Thin Flakes and Their Porous Aggregate. *Chem. Mater.* **1997**, *9*, 602−608.

(13) Sasaki, T. Molecular Nanosheets of Quasi-TiO_2: Preparation and Spontaneous Reassembling. *Supramol. Sci.* **1998**, *5*, 367−371.

(14) Sasaki, T.; Watanabe, M. Osmotic Swelling to Exfoliation. Exceptionally High Degrees of Hydration of a Layered Titanate. *J. Am. Chem. Soc.* **1998**, *120*, 4682−4689.

(15) Tanaka, T.; Ebina, Y.; Takada, K.; Kurashima, K.; Sasaki, T. Oversized Titania Nanosheet Crystallites Derived from Flux-grown Layered Titanate Single Crystals. *Chem. Mater.* **2003**, *15*, 3564−3568.

(16) Besselink, R.; Stawski, T. M.; Castricum, H. L.; Blank, D. H. A.; ten Elshof, J. E. Exfoliation and Restacking of Lepidocrocite-type Layered Titanates Studied by Small-angle X-ray Scattering. *J. Phys. Chem. C* **2010**, *114*, 21281−21286.

(17) Ma, R. Z.; Sasaki, T. Nanosheets of Oxides and Hydroxides: Ultimate 2D Charge-Bearing Functional Crystallites. *Adv. Mater.* **2010**, *22*, 5082−5104.

(18) Coleman, J. N.; Lotya, M.; O'Neill, A.; Bergin, S. D.; King, P. J.; Khan, U.; Young, K.; Gaucher, A.; De, S.; Smith, R. J.; Shvets, I. V.; Arora, S. K.; Stanton, G.; Kim, H.-Y.; Lee, K.; Kim, G. T.; Duesberg, G. S.; Hallam, T.; Boland, J. J.; Wang, J. J.; Donegan, J. F.; Grunlan, J. C.; Moriarty, G.; Shmeliov, A.; Nicholls, R. J.; Perkins, J. M.; Grieveson, E. M.; Theuwissen, K.; McComb, D. W.; Nellist, P. D.; Nicolosi, V. Two-Dimensional Nanosheets Produced by Liquid Exfoliation of Layered Materials. *Science* **2011**, *331*, 568−571.

(19) Nicolosi, V.; Chhowalla, M.; Kanatzidis, M. G.; Strano, M. S.; Coleman, J. N. Liquid Exfoliation of Layered Materials. *Science* **2013**, *340*, 1226419.

(20) Sasaki, T.; Ebina, Y.; Kitami, Y.; Watanabe, M.; Oikawa, T. Two-Dimensional Diffraction of Molecular Nanosheet Crystallites of Titanium Oxide. *J. Phys. Chem. B* **2001**, *105*, 6116−6121.

(21) Sasaki, T.; Watanabe, M.; Hashizume, H.; Yamada, H.; Nakazawa, H. Macromolecule-like Aspects for a Colloidal Suspension of an Exfoliated Titanate. Pairwise Association of Nanosheets and Dynamic Reassembling Process Initiated from It. *J. Am. Chem. Soc.* **1996**, *118*, 8329−8335.

(22) Maluangnont, T.; Matsuba, K.; Geng, F.; Ma, R.; Yamauchi, Y.; Sasaki, T. Osmotic Swelling of Layered Compounds as a Route to Producing High-Quality Two-Dimensional Materials. A Comparative Study of Tetramethylammonium versus Tetrabutylammonium Cation in a Lepidocrocite-type Titanate. *Chem. Mater.* **2013**, *25*, 3137−3146.
(23) Akatsuka, K.; Haga, M.-a.; Ebina, Y.; Osada, M.; Fukuda, K.; Sasaki, T. Construction of Highly Ordered Lamellar Nanostructures through Langmuir−Blodgett Deposition of Molecularly Thin Titania Nanosheets Tens of Micrometers Wide and Their Excellent Dielectric Properties. *ACS Nano* **2009**, *3*, 1097−1106.
(24) Yamaki, T.; Asai, K. Alternate Multilayer Deposition from Ammonium Amphiphiles and Titanium Dioxide Crystalline Nanosheets Using the Langmuir−Blodgett Technique. *Langmuir* **2001**, *17*, 2564−2567.
(25) Yamaki, T.; Shinohara, R.; Asai, K. Formation of Hybrid Monolayers and Langmuir−Blodgett-type Multilayers from Ammonium Cations and TiO_2 Crystalline Nanosheets. *Thin Solid Films* **2001**, *393*, 154−160.
(26) Saruwatari, K.; Sato, H.; Kogure, T.; Wakayama, T.; Iitake, M.; Akatsuka, K.; Haga, M.; Sasaki, T.; Yamagishi, A. Humidity-sensitive Electrical Conductivity of a Langmuir-Blodgett Film of Titania Nanosheets: Surface Modification as Induced by Light Irradiation under Humid Conditions. *Langmuir* **2006**, *22*, 10066−10071.
(27) Muramatsu, M.; Akatsuka, K.; Ebina, Y.; Wang, K.; Sasaki, T.; Ishida, T.; Miyake, K.; Haga, M.-a. Fabrication of Densely Packed Titania Nanosheet Films on Solid Surface by Use of Langmuir−Blodgett Deposition Method without Amphiphilic Additives. *Langmuir* **2005**, *21*, 6590−6595.
(28) Tanaka, T.; Fukuda, K.; Ebina, Y.; Takada, K.; Sasaki, T. Highly Organized Self-Assembled Monolayer and Multilayer Films of Titania Nanosheets. *Adv. Mater.* **2004**, *16*, 872−875.
(29) Sasaki, T.; Komatsu, Y.; Fujiki, Y. A New Layered Hydrous Titanium Dioxide $H_xTi_{2-x/4}O_4 \bullet H_2O$. *Chem. Commun.* **1991**, 817−818.
(30) Bras, W.; Dolbnya, I. P.; Detollenaere, D.; van Tol, R.; Malfois, M.; Greaves, G. N.; Ryan, A. J.; Heeley, E. Recent Experiments on a Small-angle/wide-angle X-ray Scattering Beam Line at the ESRF. *J. Appl. Crystallogr.* **2003**, *36*, 791−794.
(31) Sasaki, T.; Watanabe, M. Semiconductor Nanosheet Crystallites of Quasi-TiO_2 and Their Optical Properties. *J. Phys. Chem. B* **1997**, *101*, 10159−10161.
(32) Pagsberg, P.; Christensen, H.; Rabani, J.; Nilsson, G.; Fenger, J.; Nielsen, S. O. Far-ultraviolet Spectra of Hydrogen and Hydroxyl Radicals from Pulse Radiolysis of Aqueous Solutions. Direct Measurement of the Rate of H + H. *J. Phys. Chem.* **1969**, *73*, 1029−1038.
(33) Nielsen, S. O.; Michael, B. D.; Hart, E. J. Ultraviolet Absorption Spectra of Hydrated Electrons, Hydrogen, Hydroxyl, Deuterium, and Hydroxyl-d Radicals from Pulse Radiolysis of Aqueous Solutions. *J. Phys. Chem.* **1976**, *80*, 2482−2488.
(34) Yuan, H.; Besselink, R.; Liao, Z.; ten Elshof, J. E. The Swelling Transition of Lepidocrocite-type Protonated Layered Titanates into Anatase under Hydrothermal Treatment. *Sci. Rep.* **2014**, *4*, 4584.
(35) Liu, Z.-h.; Ooi, K.; Kanoh, H.; Tang, W.-p.; Tomida, T. Swelling and Delamination Behaviors of Birnessite-Type Manganese Oxide by Intercalation of Tetraalkylammonium Ions. *Langmuir* **2000**, *16*, 4154−4164.